Astron. & Astrophys. 33, 191—194 (1974)

The Dynamics of Circum-solar Dust Grains

Ph. L. Lamy

Cornell University, Ithaca, N.Y. and Laboratoire d'Astronomie Spatiale, Marseille

Received October 26, 1973

Summary. The inward spiraling of interplanetary dust grains under the Poynting-Robertson and corpuscular pressure drags is shown to be either counterbalanced or reduced by the effect of the net increase of the radiation pressure force caused by the decrease of the grains' radii when sublimating. Precise trajectories, obtained for the first time, show that silicate grains remain in the vicinity of the Sun where they describe an impressive number of orbits. Dynamical dust-free zones are clearly established and the location of regions of probable concentration are predicted; infrared emission spectra show remarkable features which can serve as signatures for the nature of the dust. It is also concluded that grains whose radii are less than about 0.2 μm play a negligible rôle in the F-corona.

Key words: interplanetary dust – F-corona – circumstellar envelopes – infrared spectrum

Introduction

The recent solar eclipse of June 30, 1973 has seen a record number of infrared observations of the corona, among which the one carried aboard the supersonic aircraft Concord was the most publicized. They were all set up to detect thermal emission from the interplanetary dust forming the F-corona and so to confirm, improve and complete the past results of Peterson (1967) and McQueen (1968). However, theoretical predictions pertinent to this problem remain rather qualitative (Belton, 1967) or simplified (Peterson, 1963). In his most authoritative article, Kaiser (1970) made considerable approximations in order to avoid using Mie theory to solve for the interaction of dust grains with the solar radiation field. He had a correct insight into the dynamical behavior of the dust, but was unable to calculate their trajectories. The results presented here, based on recent calculations of Mie scattering by various materials, cast a new light on the dynamics of the F-corona and lead to very definite predictions about its structure and emission spectrum. It is hoped that these results will lead to fruitful confrontation with recent observations.

Interaction with the Solar Radiation Field

The key to the problem of the dynamics of the interplanetary dust lies in the determination of all its interactions with the interplanetary medium. In order to do this, I considered spherical models of obsidian, andesite and iron grains with radii lying in the micron and submicron range. The choice of these materials – two silicates and a metal – rests on two grounds. First, one generally considers materials of dielectric and metallic types for a study of this kind. In this respect, silicates and iron are the archetypes and are favored because of their predicted elemental abundances. Obsidian, a volcanic glass, represents a good example of dirty fused quartz – much more realistic than pure crystalline quartz whose existence is questionable in interplanetary space – while andesite, a rock close to the olivine family, is representative of stony meteorites. Second, their optical properties are reasonably well known over a large spectral range thanks to the recent measurements of Pollack *et al.* (1973) for obsidian and andesite – the chemical composition of their specimens is reproduced here in Table 1 – and of Yolken and

Table 1. Chemical composition of the obsidian and andesite samples (from Pollack *et al.*, 1973)

	Obsidian	Andesite
SiO_2	76.20	54.15
Al_2O_3	13.06	16.49
Fe_2O_3	0.41	2.56
FeO	0.60	4.96
MgO	0.12	6.04
CaO	0.44	7.13
Na_2O	4.41	3.73
K_2O	3.91	2.02
H_2O^+	0.26	1.06
H_2O^-	0.1	0.11
CO_2	0.08	0.16
TiO_2	0.09	1.03
P_2O_5	0.02	0.29
MnO	0.14	0.14
BaO	0.074	0.052

Kruger (1965) and Lenham and Treherne (1968) for iron. The knowledge of the complex index of refraction $m = n - ik$ as a function of wavelength λ has allowed me to evaluate the efficiency factors for absorption Q_{abs} and radiation pressure Q_{pr} (to appear in a forthcoming paper) for seven values of the grains' radius s ranging from 0.05–1 μm and for the following spectral ranges:

obsidian: 0.2 – 50 μm (152)

andesite: 0.2 – 50 μm (152)

iron: 0.2 – 18 μm (124).

Appearing in parentheses is the total number of values of λ for which the computations have been carried out and which illustrates the accuracy of the method. The radiation pressure force F_p and the temperature distribution T_g of the grains are given by the equations:

$$F_p = s^2 \frac{\Omega}{c} \int_0^\infty Q_{pr}(m, \lambda) F_\odot(\lambda)\, d\lambda$$

$$\frac{\Omega}{\pi} \int_0^\infty Q_{abs} F_\odot(\lambda)\, d\lambda = 4 \left[\int_0^\infty Q_{abs} B(\lambda, T_g)\, d\lambda + \frac{dE}{dt} L_s(T_g) \right]$$

where Ω is the solid angle subtended by the Sun at the point where the grain is located, c is the velocity of light, $F_\odot(\lambda)$ is the monochromatic emissive power (or flux) of the Sun, $B(\lambda, T_g)$ is Planck's function, $L_s(T_g)$ is the latent heat of sublimation of the material. dE/dt, the mass sublimation rate, can be expressed in terms of the rate of decrease of s, ds/dt, a quantity which will be given later, as:

$$\frac{dE}{dt} = \delta \left| \frac{ds}{dt} \right|$$

where δ is the density of the material. The details of these computations and the complete results will appear in a forthcoming paper. For our present purpose, I plotted β, the ratio of F_p to the gravitational force F_g, against s in Fig. 1 and summarized the temperature distribution of the grains $s \simeq 1$ μm close to the Sun by the following approximations:

$T = 3227.6\, R^{-1.03}$ for obsidian,

$T = 6611.7\, R^{-0.72}$ for andesite,

$T = 4025\, R^{-0.425}$ for iron,

where R is the heliocentric distance in units of solar radii ($R_\odot$) and T is expressed in degrees Kelvin. It is interesting to note that β remains well below the critical value of 1 except in a narrow range for iron.

As the grains approach the Sun, increasing temperature cause them to be eroded by sublimation and even completely destroyed long before they could reach their melting point. The rate of decrease of s is found to be (Lamy, 1973):

$$\frac{ds}{dt} = -408 (p/\delta) \sqrt{(M/T)} \quad \mu m/s$$

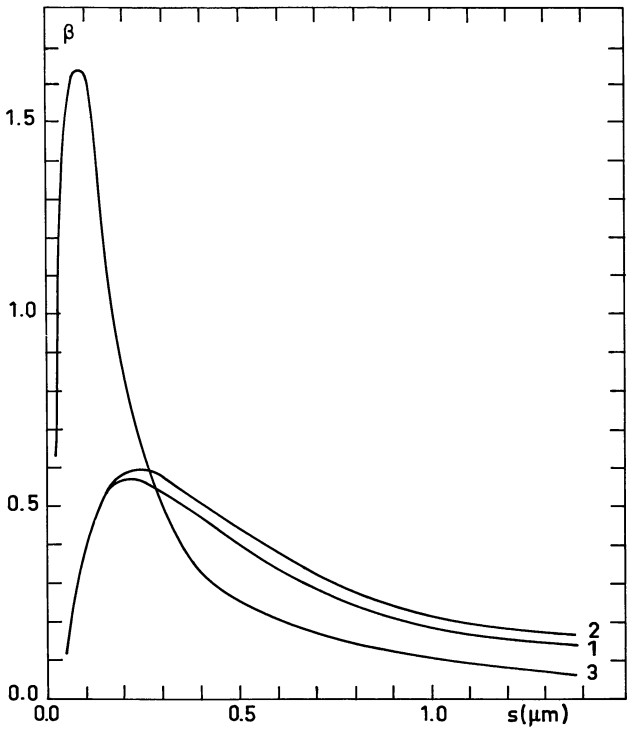

Fig. 1. The ratio β for spheres of obsidian (1), andestie (2) and iron (3) as a function of their radii s

where p is the vapor pressure of the material in tor, δ its density in gm/cm^3 and M its atomic or molecular mass. Finally the expression of the Poynting-Robertson (P–R) drag follows immediately from knowledge of β using the work of Guess (1962) for a finite source of radiation.

Interaction with the Solar Wind

The interaction of interplanetary grains with the solar wind is dominated by the corpuscular pressure resulting from direct impacts of, primarily, protons and α-particles. The force is found to be (Baines *et al.*, 1965):

$$\boldsymbol{F} = \pi s^2 |\boldsymbol{w} - \boldsymbol{V}| (\boldsymbol{w} - \boldsymbol{V}) \sum_{p,\alpha} m_i n_i$$

where $\boldsymbol{w}$ denotes, the wind velocity, $\boldsymbol{V}$ the grain's orbital velocity and m_i and n_i, the mass and number density of each particle species. The tangential component of $\boldsymbol{F}$, which always opposes the motion, amounts to approximately 50% of the P–R drag while its radial component remains negligible. The plasma or Coulomb drag, due to Coulomb collisons with solar wind particles, was thoroughly investigated by means of the Fokker-Planck theory and found to be unimportant for this problem (Lamy, 1973). Sputtering by solar wind ions was studied using the theory of Rol *et al.* (1960) and was found to be far less destructive than sublimation in the coronal region (Lamy, 1973). Lack of sufficient knowledge of grain potentials and magnetic fields in

the corona unfortunately prevents any meaningful estimation of possible electromagnetic interactions for the time being.

Dynamics of Dust Grains

The dynamical effects of the P–R and corpuscular drags result in the well known circularization $\left(\frac{de}{dt}<0\right)$ and inward spiraling $\left(\frac{da}{dt}<0\right)$ of the orbit; here e is the eccentricity and a the semi-major axis of the orbit. Sublimation changes the relative importance of F_p with respect to F_g. If s_m denotes the value of s for which β is maximum, perturbation theory shows that for

$$s>s_m\left(\frac{d\beta}{ds}<0\right) \quad \text{then} \quad \frac{de}{dt}>0 \quad \text{and} \quad \frac{da}{dt}>0,$$

$$s<s_m\left(\frac{d\beta}{ds}>0\right) \quad \text{then} \quad \frac{de}{dt}<0 \quad \text{and} \quad \frac{da}{dt}<0.$$

In the first case, $s>s_m$, there is thus a competitive process the result of which depends upon the relative importance of the opposing effects. It is very likely that interplanetary grains reach the coronal region on almost circular orbits slowly spiraling toward the Sun under the influence of the drags. As sublimation becomes more and more efficient, the grains for which $s>s_m$, have their inward motion slowed down, possibly stopped, and their orbits become elliptic. If the size of the orbits increases, sublimation is reduced, the grains recede under the effect of the drags, and so on. In contradiction with previous theories (Belton, 1967; Kaiser, 1970), silicate grains will not leave the solar system ($\beta<1$); instead, they will remain in a well defined "equilibrium" zone. I have numerically integrated the equations of motion to investigate in detail the dynamical behaviour of the grains and to localize possible regions of stability where thermal emissions could be detected. The computer program uses the Runge-Kutta fourth order method with automatic time increment and contains a model of the solar wind derived from the recent measurements of Koutchmy (1972) in order to carefully evaluate all the effects mentioned above. In all runs, a grain is injected on a circular orbit where no sublimation takes place and therefore spirals inward during many revolutions. This precaution insures that its approach to the corona is sufficiently realistic.

Starting from a heliocentric distance of $3\,R_\odot$ (on a circular orbit), a typical obsidian grain, 1 μm in radius, gently spirals inward during 30 revolutions and reaches $2.4\,R_\odot$ with negligible erosion. The orbit becomes elliptic and shrinks slowly for a few revolutions. While the perihelion distance R_p keeps decreasing very slowly to a minimum of $2.2\,R_\odot$, the aphelion distance R_a starts to increase so that it reaches $3.52\,R_\odot$ at the fiftieth revolution ($s=0.455$ μm). This process accelerates during the following two revolutions and R_a amounts to $5.5\,R_\odot$. But now $s<s_m$, circularization takes place and the next aphelion is located at $3.35\,R_\odot$. Thereafter, the grain completely evaporates in less than one orbital period. Such grains thus remain in the region extending from 2.2–3.5 $R_\odot$, the lower limit defining the edge of the dust-free zone. At a typical distance of $2.4\,R_\odot$ where the inward spiraling ceases, the temperature reaches 1310 °K. Figure 2 illustrates the emission spectrum, as predicted by Mie theory, of a 1 μm spherical grain at 1200 and 1400 °K. They do not differ much and reflect the reststrahlen band structure of obsidian with its two characteristic absorption bands at 3 and 9.2 μm. Such features should facilitate the detection of obsidian type dust in the F-corona.

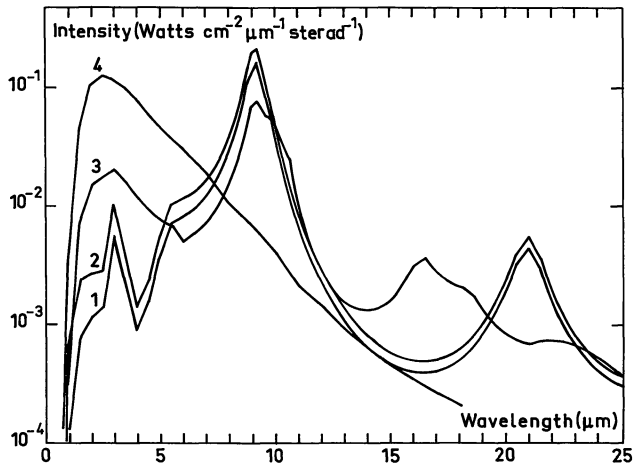

Fig. 2. The emission spectra of 1 μm spheres of obsidian at 1200 °K (1) and 1400 °K (2), of andesite (3) and of iron (4), both at 1000 °K

Andesite grains exhibit a different behaviour: a typical 1 μm grain, located at $16\,R_\odot$, must reach $14.5\,R_\odot$ after about 100 revolutions ($s=0.87$ μm) before its orbit starts to become elliptic. Its eccentricity slowly increases while its overall size keeps decreasing so that $R_a=11.05$ and $R_p=11.02$ at the 300th revolution ($s=0.546$ μm). At the 367th, the orbit is rapidly becoming circular ($s<s_m$) at a mean distance of $10.2\,R_\odot$; the grain travels five more orbits before being completely destroyed. Such grains are thus likely to be found in a broad region extending from 10.8–14.5 $R_\odot$ approximately, with an absolute lower limit of $10.2\,R_\odot$. Corresponding temperatures reach 1000 °K (1050 °K at $12.88\,R_\odot$) which gives the emission spectrum of a 1 μm spherical grain as illustrated on Fig. 2. The double hump feature is more pronounced than for obsidian, although it reflects the same band structure.

An iron grain, 1 μm in radius, starting from $25\,R_\odot$, spirals inward until it reaches $24.45\,R_\odot$ after 100 revolutions ($s=0.83$ μm). The orbit becomes slowly elliptic, decreases to a mean distance of $24.35\,R_\odot$, and then starts to expand very slowly so that, at the 300th

orbit, $R_a = 25.16$ and $R_p = 25.09\ R_\odot$. The 450th revolution witnesses the beginning of a wild increase of the aphelion distance while that of the perihelion decreases slightly. After about 600 revolutions, $s = 0.2\,\mu m$ and the ellipse as a whole resumes its expansion; the orbit crosses that of the Earth at the 640th revolution. The integration was stopped eight orbits later with $s = 0.1835\,\mu m$, $R_a = 505\ R_\odot = 2.35$ AU and $R_p = 51\ R_\odot$. The grain may eventually leave the solar system. The limit of the dust-free zone for iron grains can be taken as $24.3\ R_\odot$ approximately while a zone of stability is observed around $24.35\ R_\odot$, corresponding to a temperature of 1036 °K.

Figure 2 illustrates the emission spectrum of an iron grain at 1000 °K; it ressembles that of a black-body because of the continuous absorption spectrum of iron.

Discussion

These results call for further comment; first, this behaviour is typical of grains for which $s > s_m$, with different time-scales depending upon the initial radii. Whenever $s < s_m$, the grains keep spiraling inward and last only a very short time; in summary, grains whose radius is less than approximately 0.2 μm play a negligible rôle in the F-corona. It should be clear that the dynamical features depend fundamentally upon the optical properties of the material, as they govern the shape of the function $\beta(s)$ as well as the temperature distribution (through the absorption spectrum) and, in turn, $\frac{ds}{dt}$. The resulting spatial segregation between grains of different compositions is enormous and thus of utmost observational importance. However, materials having some "intermediate" absorption spectrum (the sublimation properties do not vary much) will remain in some intermediate regions. Present evidence of thermal emission at $3.5–4\ R_\odot$ (Peterson, 1967; McQueen, 1968) favours an obsidian type material behaving as explained above. Belton (1967) has pointed out that regions where the inward spiraling is slowed down and reversed, correspond to regions of concentration when considering a cloud of grains. This leads to a reinforcement of the thermal emission and improves the chance of detection. The interactions discussed above have no influence on the inclination of the grains' orbits, so that this parameter keeps its initial value. Therefore, the question of possible concentration of dust near the ecliptic plane (McQueen, 1968) is still open. Finally, it is clear that past evaluations of the rate of destruction of the zodiacal cloud by Wyatt and Whipple (1950) and Carpenter and Pastusek (1967), which take into account the drag only, need to be completely revised on the basis of the present results.

Acknowledgement. I thank J. Burns, S. Koutchmy and J. C. Pecker for interesting discussions and J. Caplan for revision of the manuscript. The hospitality of the Service d'Aéronomie du C.N.R.S., where the computations were carried out, is gratefully acknowledged.

References

Baines, M. J., Williams, I. P., Asebiomo, A. S. 1965, *Monthly Notices Roy. Astron. Soc.* **130**, 63
Belton, M. J. S. 1967, NASA SP-150, 301
Carpenter, D. G., Patusek, R. R. 1967, *Planet. Space Sci.* **15**, 593
Guess, A. W. 1962, *Astrophys. J.* **135**, 855
Kaiser, C. B. 1970, *Astrophys. J.* **159**, 77
Koutchmy, S. 1972, *Solar Phys.* **24**, 373
Lamy, P. L. 1973, Doctoral Thesis, Cornell University
Lenham, A. P., Treherne, D. M. 1968, *J. Opt. Soc. Am.* **56**, 1137
McQueen, R. M. 1968, *Astrophys. J.* **154**, 1059
Peterson, A. W. 1963, *Astrophys. J.* **138**, 1218
Peterson, A. W. 1967, *Astrophys. J. Letters* **148**, L 37
Pollack, J. B., Toon, O. B., Khare, B. N. 1973, *Icarus* **19**, 372
Wyatt, S. P., Whipple, F. L. 1950, *Astrophys. J.* **111**, 134
Yolken, H. T., Kruger, J. 1965, *J. Opt. Soc. Am.* **55**, 842

Ph. L. Lamy
Laboratoire d'Astronomie Spatiale
Traverse du Siphon
Les trois Lucs
F-13012 Marseille, France